

Comparison of IRI-2012 with JASON-1 TEC and incoherent scatter radar observations during the 2008–2009 solar minimum period



Eun-Young Ji, Geonhwa Jee*, Changsup Lee

Division of Climate Change, Korea Polar Research Institute, Incheon, South Korea

ARTICLE INFO

Article history:

Received 23 March 2016

Received in revised form

20 May 2016

Accepted 21 May 2016

Available online 24 May 2016

Keywords:

IRI

Solar minimum

JASON-1 TEC

ABSTRACT

The 2008–2009 solar minimum period was unprecedentedly deep and extended. We compare the IRI-2012 with global TEC data from JASON-1 satellite and with electron density profiles observed from incoherent scatter radars (ISRs) at middle and high latitudes for this solar minimum period. Global daily mean TECs are calculated from JASON-1 TECs to compare with the corresponding IRI TECs during the 2008–2009 period. It is found that IRI underestimates the global daily mean TEC by about 20–50%. The comparison of global TEC maps further reveals that IRI overall underestimates TEC for the whole globe except for the low-latitude region around the equatorial anomaly, regardless of season. The underestimation is particularly strong in the nighttime winter hemisphere where the ionosphere seems to almost disappear in IRI. In the daytime equatorial region, however, the overestimation of IRI is mainly due to the misrepresentation of the equatorial anomaly in IRI. Further comparison with ISR electron density profiles confirms the significant underestimation of IRI at night in the winter hemisphere.

© 2016 Elsevier Ltd. All rights reserved.

1. Introduction

The International Reference Ionosphere (IRI) is the most widely used standard model for the ionospheric specifications. It is an international joint project of the Committee on Space Research (COSPAR) and the International Union of Radio Science (URSI). The IRI, as a data-driven empirical model, provides the total electron content (TEC) for a given location, time, and date as well as the height profiles of electron density, electron temperature, and ion composition (Bilitza and Reinisch, 2008; Bilitza et al., 2014 and references therein).

The 2008–2009 solar minimum period was unusual in terms of solar EUV and its duration. The level of solar EUV was extremely low and the duration of low solar activity was longer than any previous minimum periods (Russell et al., 2010; Solomon et al., 2010; Chen et al., 2011). The anomalous characteristics in solar EUV level lead to the unique state of the ionosphere as well as the thermosphere during the last solar minimum period (Liu et al., 2011; Emmert et al., 2010; Solomon et al., 2010, 2011, 2013; Jee et al., 2014).

A number of studies have evaluated how the IRI estimates the ionosphere during the unusual solar minimum period (Lühr and Xiong, 2010; Klenzing et al., 2011; Bilitza et al., 2012; Lee and Reinisch, 2012; Araujo-Pradere et al., 2013; Yue et al., 2013;

Zakharenkova et al., 2013; Themens et al., 2014; Zakharenkova et al., 2015). Most of these studies seem to indicate that the IRI is not capable of correctly reproducing the ionosphere during this period. For example, Klenzing et al. (2011) compared the IRI-2007 with ion density profiles observed from C/NOFS satellite near the magnetic dip equator for the December solstice of 2008. They found that the IRI overestimates the ion density at 400–850 km altitude in the afternoon and post-sunset local time sector. Lühr and Xiong (2010) compared the IRI-2007 with electron densities observed from CHAMP and GRACE satellites for 2008 and 2009. They found that the IRI on average overestimates the electron density at 400–500 km altitude by about 50% and 60% for 2008 and 2009, respectively. By using ionosonde and C/NOFS satellite data, Bilitza et al. (2012) further investigated the limitations of IRI-2007 for the topside ionosphere, reported by Lühr and Xiong (2010), during the last solar minimum period. Based on the results of the comparisons with data for NmF2 and topside electron density at 400–500 km altitude, they investigated the possible causes for the IRI overestimation of the topside density despite the good agreement of IRI NmF2 with ionosonde observations. Most recently, Themens et al. (2014) evaluated the performance of IRI-2007 within the polar cap using the ionosonde measurements at four Canadian High Arctic Ionospheric Network (CHAIN) stations during the solar minimum period between 2008 and 2010. Their results showed that the IRI significantly underestimates nighttime NmF2 in the polar cap for most seasonal conditions except for summer period.

Most of previous evaluation studies of the IRI during the 2008–

* Corresponding author.

E-mail address: ghjee@kopri.re.kr (G. Jee).

2009 solar minimum period were performed in the specific regions of altitude or latitude and longitude in which only a certain type of observations are available from satellites or ground-based instruments. In this study, we use the JASON-1 TEC data for the global ionosphere and the measurements of electron density profiles obtained from the incoherent scatter radars at middle and high latitudes, in order to see how IRI-2012 performs for the global ionospheric TEC and the height profiles of electron density during the solar minimum period.

2. Data and model

2.1. JASON-1 TEC data

JASON-1 is the satellite mission developed jointly by the Centre National d'Etudes Spatiales (CNES), France and the National Aeronautics and Space Administration (NASA), USA and launched in December 2001, as the TOPEX/Poseidon follow-on mission to monitor the surface of the global ocean (Ping et al., 2004). The precise sea surface height measurement requires the removal of the ionospheric delay imposed on the altimeter, which results in, as a by-product of the satellite mission, the TEC measurements of the ionosphere between the sea surface and the satellite orbit altitude of about 1336 km (Fu et al., 1994; Imel, 1994). As in the TOPEX satellite, the TEC data from JASON-1 satellite provides a measurement of the ionospheric vertical TEC almost every second but only over the ocean with 66° inclination.

TEC data from the Global Positioning System (GPS) is the most widely utilized TEC measurement for the ionosphere due to the unprecedented temporal and spatial coverages of the observation. However, there are fundamental limitations in the GPS TEC data due to the characteristics of the measurement. First, apart from the instrumental biases of GPS satellites and ground-receivers, the GPS TEC measurement initially produces slant TECs along the line-of-sight path between the satellites and receivers and the slant TECs need to be converted to vertical TECs, typically based on the assumption of a thin shell model of the ionospheric electron content situated at a certain altitude. This procedure undoubtedly introduces errors in the resulting vertical TECs, especially when the horizontal gradient of the ionospheric density is large as in the regions of the equatorial anomaly and auroral oval or at dusk sector (Mannucci et al., 1998). The another aspect of the GPS TEC measurement is that it includes not only the ionospheric electron contents but also the plasmaspheric electron content within the satellite orbit altitude of 20,200 km. The plasmaspheric contribution to GPS TEC cannot be ignored, especially at night and it can even reach as much as the ionospheric contribution in the early morning sector (Yizengaw et al., 2008; Jee et al., 2010; Lee et al., 2013).

On the other hand, the TOPEX and JASON (T/J) TEC measurements provide the most direct estimate of the ionospheric vertical TEC between the ground and the satellite orbit of about 1336 km over the global oceans, without any additional procedures for the vertical TEC. Furthermore, the altitude range for T/J TEC is hardly affected by plasmaspheric processes. In principle, therefore, it is supposed to produce the most direct and accurate TEC measurement of the ionosphere. Most of validation studies for T/J TEC measurements have been performed by comparisons with TEC measurements from GPS and DORIS (Doppler orbitography and radiopositioning integrated by satellite) and TEC models based on these data (Imel, 1994; Ho et al., 1997; Codrescu et al., 2001; Ping et al., 2004; Zhao et al., 2004; Brunini et al., 2005; Azpilicueta and Brunini, 2009; Yasyukevich et al., 2010).

DORIS TEC is measured by a receiver onboard the TOPEX satellite, which produces the slant TEC between the satellite and a

global set of DORIS beacons spread around the Earth. This TEC is basically similar to GPS TEC except that it has the same altitude range as T/J TEC measurements. Ideally, DORIS TEC would be the most favorable independent data to validate T/J TEC. However, DORIS TEC measurements involve more complex preprocessing steps to derive the vertical TECs from DORIS phase measurements than GPS TEC observation (Imel, 1994; Zlotnicki, 1994; Dettmering et al., 2014). In particular, Zlotnicki (1994) demonstrated in their analysis of the altimetric corrections in TOPEX that the ionospheric correction by the TOPEX dual-frequency altimeter is superior to the DORIS correction.

In the comparison of T/J TEC with GPS TEC, they mostly utilized the global TEC models such as the Global Ionosphere Map (GIM) which should have additional model uncertainties in addition to all the limitations of GPS TEC measurement. Furthermore, the GPS TEC-driven models show the worst performance in the oceans where the GPS receivers are scarce. Note that the T/J TEC measurements exist only over the oceans. Using GPS TECs from the regional receiver network with high spatial resolution in Japan, Ping et al. (2004) reported that the bias between JASON-1 and GPS TECs is not significant, less than 1 TECU. Although a number of previous study indicated that there seems to be a systematic bias of a few TECUs in the T/J TEC measurements (Ho et al., 1997; Codrescu et al., 2001; Brunini et al., 2005), most of these studies is only showing that there are a few TECU differences between the measurements, but their results do not necessarily prove which measurement is more accurate than the other measurements. Since there are no known issues in the T/J TEC determination and no previous studies clearly demonstrating that the T/J TECs have a bias, based on the comparison with valid independent observations for the ionospheric TEC, we use the T/J TEC data as a ground truth to evaluate the IRI model (Yasyukevich et al., 2010).

For this study, the 1-s TEC data were averaged for about 18 s, which corresponds to about 1° of the satellite orbit, to reduce the observational random errors (Imel, 1994; Zlotnicki, 1994). For each 18-s data points, the corresponding geomagnetic coordinates are computed by adopting quasi-dipole coordinates (Richmond, 1995). For global TEC map, we bin the data in magnetic latitude (MLAT) versus magnetic local time (MLT) coordinate and the binning resolution for MLAT and MLT is 2° × 15 min. We also used three seasonal bins: equinox (day of year: 50–110 and 234–294), December solstice (day of year: 1–50 and 295–366), and June solstice (day of year: 111–233) for the seasonal variations of the ionosphere.

2.2. ISR electron density profiles

To further investigate the results of the IRI evaluation for the global ionosphere, we used electron density profiles observed by three incoherent scatter radars (ISRs) located at middle and high latitudes: Millstone Hill (42.6°N, 288.5°E, invariant latitude=55°); European Incoherent Scatter Tromsø UHF radar (EISCAT: 69.6°N, 19.2°E, invariant latitude=66°); EISCAT Svalbard radar (ESR: 78.2°N, 16.0°E, invariant latitude=75°). Table 1 shows the numbers of days available from three radars for three seasonal cases. Since the electron density profiles from ISRs are produced with an

Table 1
Numbers of days for which the ISR data are available for three seasonal cases.

	Millstone Hill	EISCAT (Tromsø)	ESR (Svalbard)
Equinox	40	62	24
Dec. Sol.	50	113	75
Jun. Sol	47	86	41
Total	117	248	174

irregular altitude step, each density profile was reproduced with a regular altitude step of 25 km to apply local time and seasonal binning as in the JASON-1 TEC data. The resulting ISR electron density profiles will be compared with the corresponding IRI density profiles.

2.3. International reference ionosphere-2012

The IRI-2012 is the latest version of the IRI model, which was improved to better estimate not only the electron density, but also electron temperature and ion composition (Bilitza et al., 2014 and references therein). In particular, the IRI-2012 includes a new model for the region between the F2 and F1 peak heights, which can have a non-negligible contribution to TEC. It also includes a representation of the auroral oval boundaries and a description of storm effects in the auroral E region but these auroral options are turned off in the standard version of IRI-2012. The standard version is the most recommended version of the IRI model by developer for a general specification of the ionosphere. This version adopts the URSI option for foF2 and NeQuick topside model. In particular, it was reported that the NeQuick topside option shows the best performance among the available options for the topside ionosphere in IRI (Bilitza, 2009). The selected options for the standard version of IRI-2012 are listed in Table 2. It should be reminded that we do not intend to evaluate the IRI estimations with different options as done by Yue et al. (2013) but will use only the estimation of the standard version of IRI in order to evaluate the overall performance of the IRI during the extremely low solar activity.

We utilized the new *ig_rz.dat* file updated in March 2013 for the 12-month running median of the ionospheric index IG12 and solar sunspot number Rz12 (Liu et al., 1983; Bilitza, 2000). Cherniak et al. (2013) performed a comparison study between ISR observations for the ionospheric parameters and the corresponding IRI predictions with various versions of *ig_rz.dat* file during the autumnal equinoxes of 2007 and 2008. They found that the best agreement with observations occurs in the IRI prediction with IG12 and Rz12 indices derived from the observational data. The IG12 and Rz12 indices updated in March 2013 include the data for the ionosphere and sunspot number during the last solar minimum periods to guarantee the best available IRI prediction for the study period.

The IRI TECs for the global TEC maps are calculated at the time of day, day of year, and location of the 18-second JASON-1 TEC data along the satellite orbit. The IRI electron density profiles are also calculated at the time of ISR observations.

3. Comparison of IRI TEC with JASON-1 TECs for the global ionosphere

For the global mean ionosphere, daily mean TECs from IRI (black) and JASON-1 satellite (gray) are presented with the day of

Table 2
Selected options for the standard version of IRI-2012.

Parameter	Standard version
Sunspot number, Rz12	<i>ig_rz.dat</i> (Mar. 2013)
Ionospheric index, IG12	<i>ig_rz.dat</i> (Mar. 2013)
Daily F10.7 index	<i>apf107.dat</i>
Ne topside	NeQuick
Te topside	TBT-2012
Ion composition	RBV-2010 & TTS-2003
F peak model	URSI
Bottomside thickness (B0, B1)	ABT-2009
foF2 storm model	On
Auroral boundary	Off
foE auroral storm model	Off

year for 2008 (top) and 2009 (bottom) in Fig. 1. This figure shows the evident underestimation of the IRI model by about 2–6 TECU, which corresponds to about 20–50% (~35% on average), as compared with the JASON-1 TEC data. The RMS errors between the two are 4.3 and 3.9 TECU for the year 2008 and 2009, respectively. The magnitude of the underestimation is mostly about 4 TECU for the most of year but it becomes smaller for the day of year 270–360 in both years. Note that the wavy structure with about 60-day period is due to the characteristics of the satellite orbit; the JASON-1 satellite orbit shifts only 2 h in local time per 10-day cycle and it takes about 6 cycles to cover an entire day of local time considering the ascending and descending passes.

Fig. 2 shows the global TEC maps for IRI (top), JASON-1 (middle), and their relative difference (bottom) in the geomagnetic latitude and magnetic local time coordinate. From the global TEC maps, we can identify the specific differences between the IRI and JASON-1 TECs. As shown in the global mean ionospheric TEC, in general, the IRI underestimates TEC over the whole globe except for the daytime low-latitude region around the equatorial anomaly. The underestimation is particularly strong, up to –80%, just before sunrise and at high latitudes during the nighttime. Around the equatorial anomaly, however, the IRI slightly overestimates TEC by up to about 30%. The overestimation of IRI in the daytime low-latitude region was also reported in the previous studies (e.g., Jee et al., 2005; Lühr and Xiong, 2010; Klenzing et al., 2011; Bilitza et al., 2012; Yue et al., 2013). In particular, Yue et al. (2013) compared the IRI-2007 model with the COSMIC slant TEC data and showed similar results for the global ionosphere; that is, IRI tends to underestimate TEC in the nighttime high-latitude region, while it slightly overestimates in the daytime equatorial region. In their comparison, however, they tested five different IRI runs with different options for the bottomside and topside ionospheres, which showed significantly different results depending on the selected options.

The overestimation of IRI at low latitude seems to be related not only to the magnitude of the electron density predicted by IRI, but also to the IRI capability of reproducing the equatorial anomaly structure. The equatorial anomaly in the IRI model shows the distinctive hemispheric asymmetry unlike in the JASON-1 TEC map, which results in the overestimations around the anomaly crests, in particular, in the northern hemisphere. Specifically, the northern equatorial anomaly peaks from IRI are wider in latitude as well as larger in magnitude than in the data (see Fig. 4a). In particular, for June solstice, the asymmetrical structure of the anomaly peaks is opposite in the model and data. These different structures of the equatorial anomaly produce the overestimation of IRI. Please also note that the anomaly completely disappears after sunset in the IRI TEC map while it remains almost until midnight in the JASON-1 TEC map. This difference appears as a slight overestimation of IRI over the magnetic equator in the evening sector, which is seen in Figs. 2 and 3.

We further investigate the differences in the global TEC maps for three different seasonal cases as shown in Fig. 3. This figure shows the global TEC maps for IRI (left column), JASON-1 (middle column) and their relative differences (right column) during equinox, December and June solstices from top to bottom panels. The IRI overestimation around the equatorial anomaly appears similar regardless of season. However, the IRI underestimation, mainly occurring at night and at higher latitudes, shows a systematic difference during solstices: the underestimation is much stronger in the winter hemisphere than in the summer hemisphere. This feature can be more evidently seen in Fig. 4a and b, which shows the latitudinal (4a) and local time (4b) variation of the densities selected at three local times and latitudinal sectors, respectively. This hemispheric difference is due to the strong underestimation of the IRI in the nighttime winter hemisphere. Note

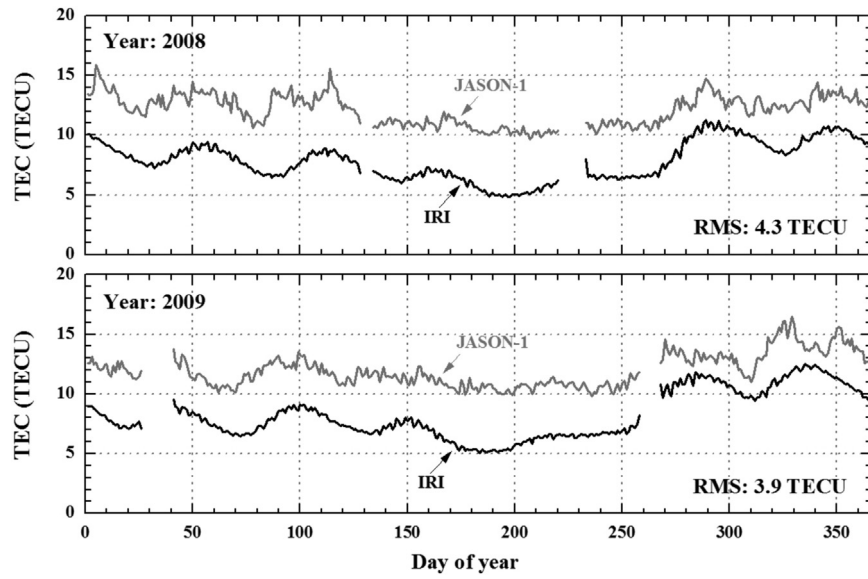


Fig. 1. The global mean TECs from IRI (black) and JASON-1 satellite (gray) are displayed for the year 2008 (top) and 2009 (bottom). The RMS errors for the comparison are 4.3 and 3.9 TECU, respectively.

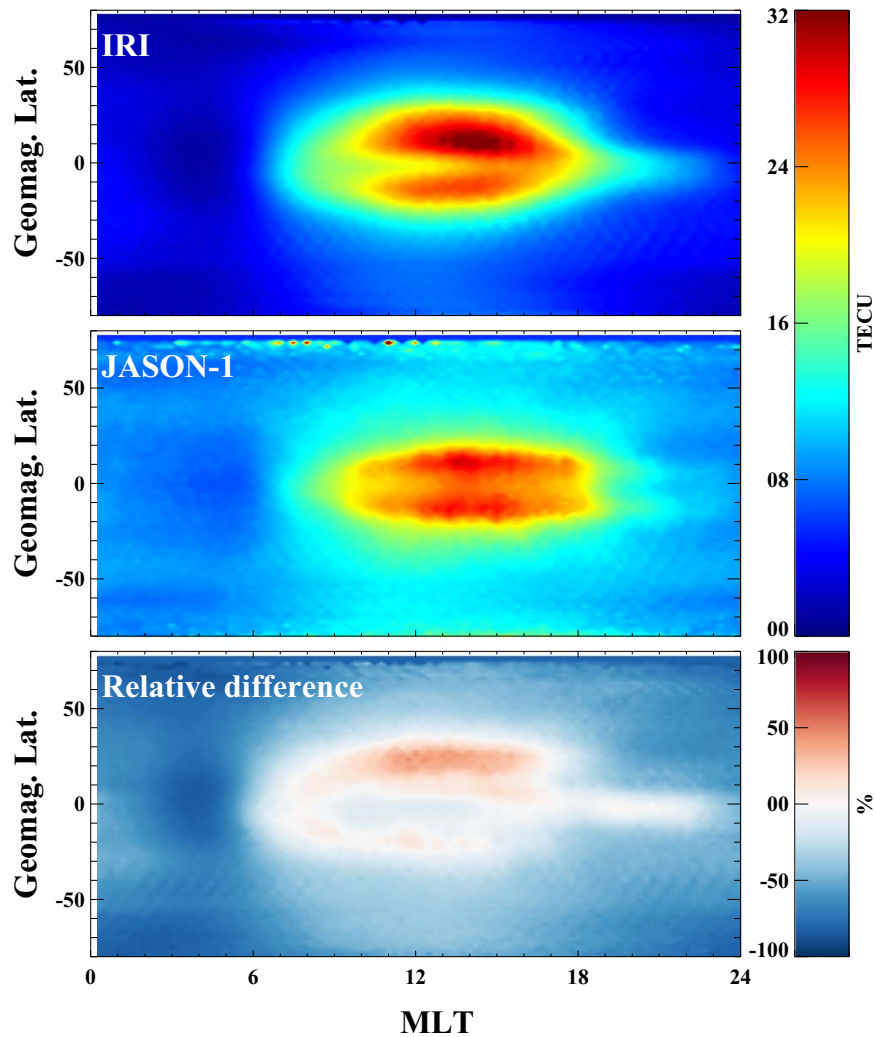


Fig. 2. The global TEC maps for IRI (top), JASON (middle) and their relative difference (bottom) are presented in the geomagnetic latitude and magnetic local time coordinate.

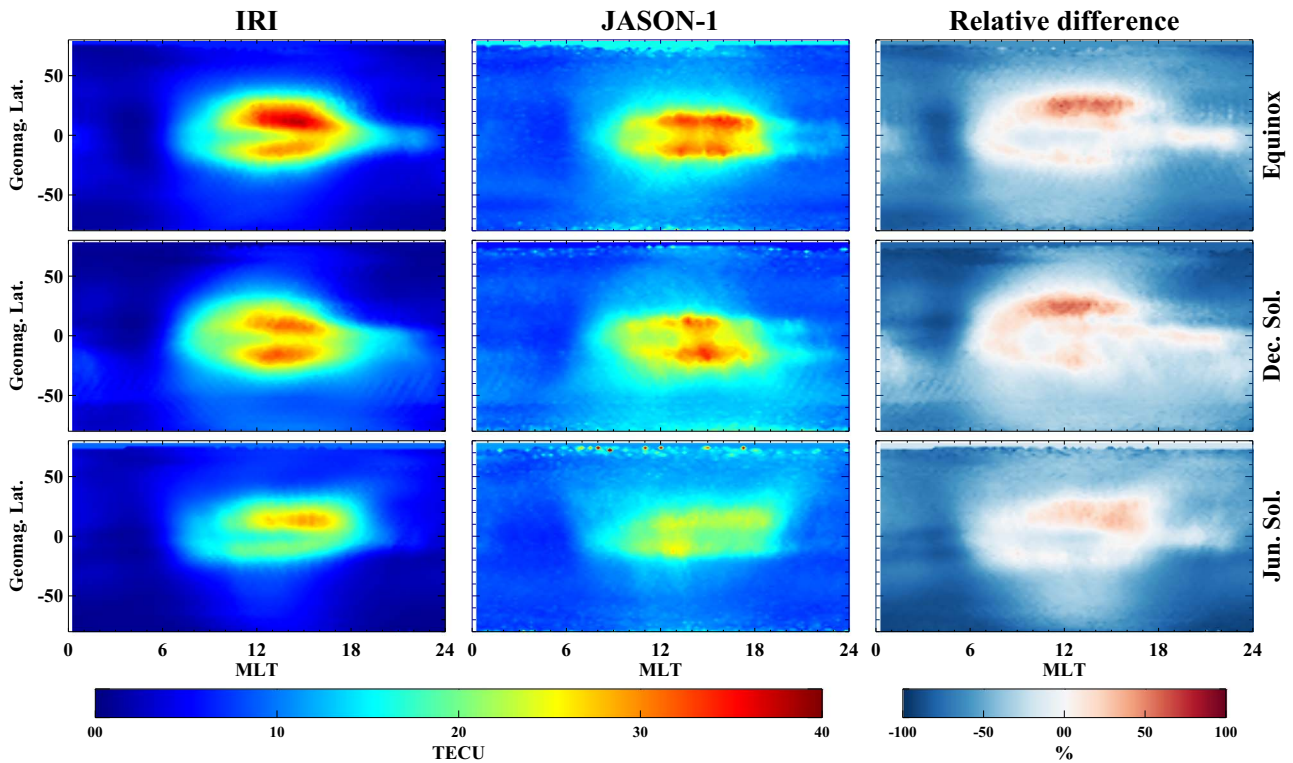


Fig. 3. The global TEC maps for IRI (left column), JASON (middle column) and their relative difference (right column) are presented for equinox, December solstice, and June solstice from top to bottom.

that the IRI nighttime TEC becomes as small as 1 TECU in the winter hemisphere (see Fig. 4b); in other words, the ionosphere in IRI seems to almost disappear in winter. Zakharenkova et al. (2015) reported that the nighttime IRI TEC in winter was extremely small, about 1 TECU at mid-latitude, compared with GPS TEC that shows values almost four times greater than IRI TEC estimation. Lühr and Xiong (2010) also made a global comparison between CHAMP electron density observation at around 350 km altitude and the corresponding IRI prediction and reported the similar result for the daytime low-latitude ionosphere, but they did not find the severe underestimation of IRI at night.

It is worth noting that the differences between IRI and JASON-1 TECs are somewhat similar to the differences between the last two solar minima reported by Jee et al. (2014) in terms of the global morphology of the differences shown in Fig. 3. Their study showed that although the daytime density during the last solar minimum was smaller than during the previous minimum period as expected, the nighttime density during the last solar minimum was actually larger than during the previous solar minimum period. This unexpected nighttime difference was greater in the winter hemisphere than in the summer hemisphere, which is similar to the result of this study that shows more severe underestimation of IRI in the nighttime winter hemisphere. They interpreted the nighttime difference due to the relative effects of the neutral composition and solar EUV production during the last solar minimum period. During the daytime, the reduced production due to smaller solar EUV is responsible for the smaller daytime density, while, at night, the reduced recombination due to cooler and reduced neutral density during the last solar minimum (Emmert et al., 2010; Solomon et al., 2011) is responsible for the larger nighttime density. At higher latitudes in the winter hemisphere, the reduced recombination is more effective, even during the daytime, than the reduced production due to large solar zenith angle. The similar differences in this comparison and Jee et al. (2014) may indicate that the empirical model like the IRI is not

able to take into account the relative effects of the reduced production and recombination.

It should be kept in mind that the comparisons between JASON-1 and IRI TECs in this study were performed only over the ocean region in which the JASON-1 TECs were measured and the corresponding IRI TECs were computed along the JASON-1 satellite orbit. Therefore, this comparison study evaluates the IRI model over the ocean where the model performance is expected to be worse than other region.

4. Comparison of IRI with ISRs electron density profiles

Using the satellite observations for the topside ionosphere during the last solar minimum, the previous studies reported that the IRI model significantly overestimates, by greater than 50%, the topside ionospheric density in the equatorial region both during the day and night (Klenzing et al., 2011; Lühr and Xiong, 2010; Bilitza et al., 2012). However, the F-region peak density in IRI is mostly in good agreement with measurements (Bilitza et al., 2012). This discrepancy indicates two possible problems in the IRI model: hmF2 or the topside shape parameter. Bilitza et al. (2012) investigated the impact of the hmF2 model within IRI on the topside ionospheric density during the last minimum period and found that there seems to be a problem in the hmF2 model within IRI, which could not represent the correct hmF2 during the unusually low solar activity.

The results of the TEC comparison in this study, however, showed that the overestimation occurs only during the daytime at around the equatorial anomaly while the nighttime IRI TEC shows significant underestimation for all latitudes. We further investigate this issue, particularly in the middle and high latitude regions by using the measurements of electron density profiles obtained from ISRs at Millstone Hill, Tromsø (EISCAT), and Svalbard (ESR). Fig. 5 shows the electron density profiles from IRI (red) and ISRs (black)

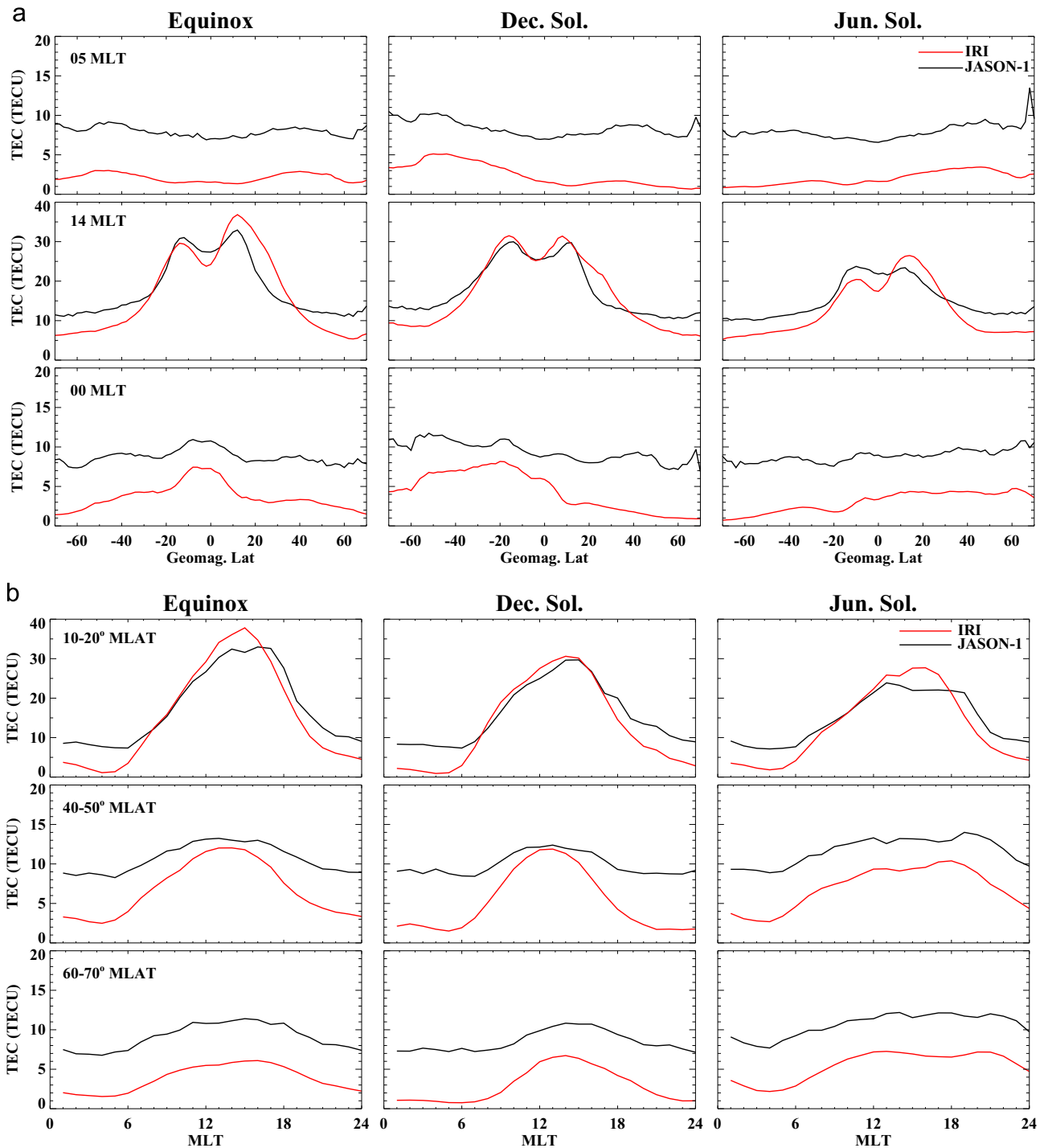


Fig. 4. a. Latitudinal variations of IRI and JASON TECs in Fig. 3 are presented at three local time sectors (05 MLT, 14 MLT, 00 MLT) for each seasonal case. b. Local time variations of IRI and JASON TECs in Fig. 3 are presented at three latitude sectors (10–20° MLAT, 40–50° MLAT, 60–70° MLAT) for each seasonal case.

for three different seasons as indicated in the figure. The daytime (14 LT) and nighttime (24 LT) density profiles are presented separately in the left and right panels, respectively. Note that there are large discrepancies at the high altitude except for Tromsø EISCAT radar. It is known that the ISR observations at high altitudes often suffer from low S/N ratio in particular for solar minimum periods when the electron density is low (Zhang and Ogawa, 2015, personal communication). Therefore, the electron density measurements from ISR may not be very reliable above about 500 km altitude for this solar minimum period.

During the day, the IRI predictions in Fig. 5 agree very well with

the ISR measurements at mid-latitude. Even at night, the density profiles around the F-region peak are in very good agreement with the measurements at mid-latitude. At higher latitudes, however, the F-region peak altitude in IRI seems to be a little higher than the measurements during the day (and the bottom thickness becomes larger in IRI), which may appear as the overestimation of IRI in the topside ionosphere, as reported for the equatorial ionosphere in the previous studies. During the night, the IRI electron density profiles greatly deviate from the ISR density profiles, in particular, at higher latitudes, which result in the smaller TECs in IRI than in the measurements. The disagreement between IRI and ISR density

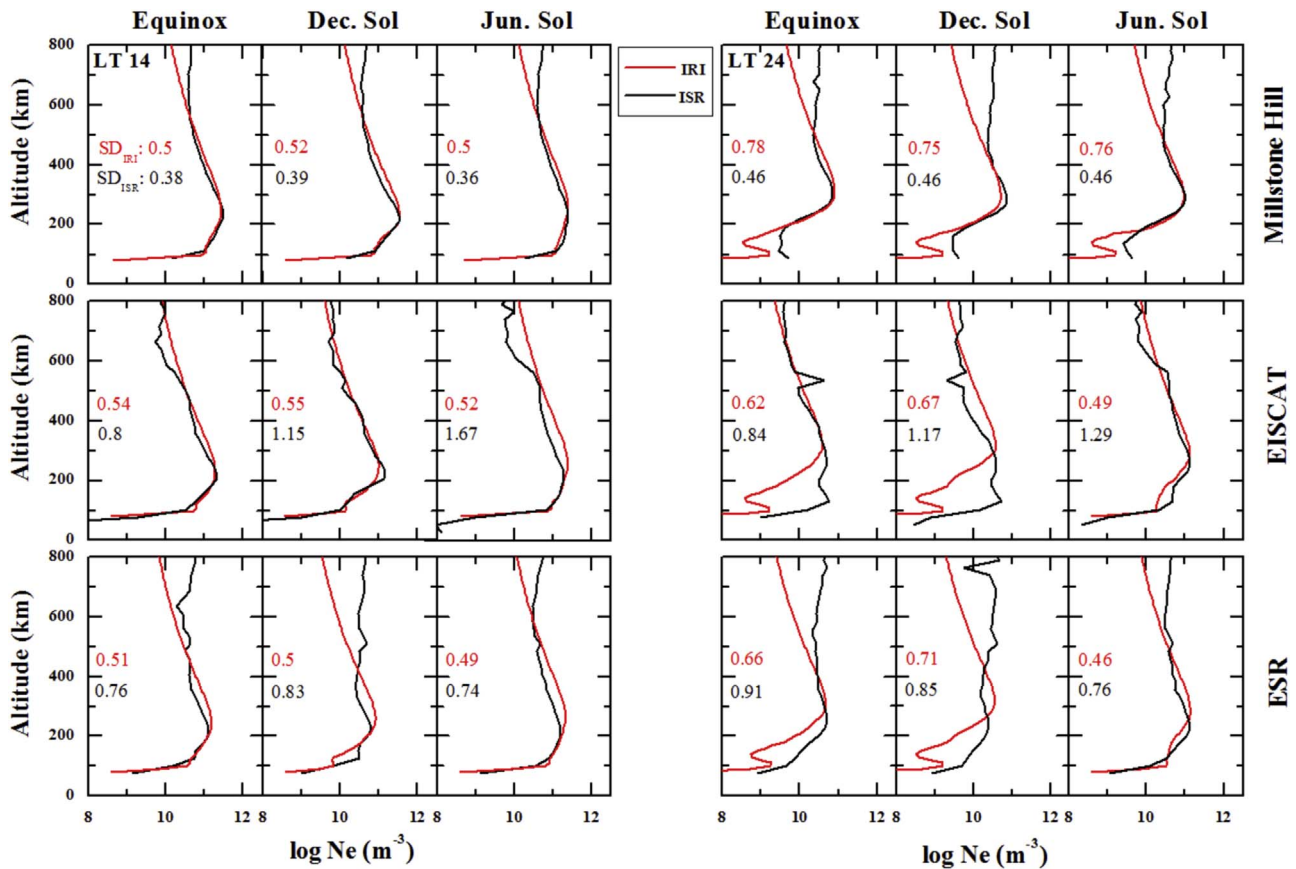


Fig. 5. Electron density profiles obtained from IRI (red) and ISR measurements (black) during the day (LT 1400) and night (LT 2400) are displayed at the left and right panels, respectively. For each local time sector, the density profiles are presented for three seasonal cases (equinox, December solstice, and June solstice) and for three different locations (Millstone Hill, Tromsø EISCAT, Svalbard ESR) as indicated. Mean standard deviations (red text: IRI and black text: ISR) of each profiles are also depicted in the figure. (For interpretation of the references to color in this figure legend, the reader is referred to the web version of this article.)

profiles at high latitudes is significant in equinox and winter while they are reasonably in good agreement in summer. Themens et al. (2014) also reported similar result for the seasonal variations of differences in their comparison between IRI-2007 NmF2 and ionosonde measurements within polar cap and auroral oval. The results of the comparison with ISR measurements confirm that the IRI model mostly underestimates the electron density at night, as found in the comparison with JASON-1 TEC measurements, especially in winter. It also indicates that there seems to be a fundamental limitation in IRI for the representation of the correct altitude profiles of electron density within the polar cap, especially in the winter hemisphere.

5. Summary and conclusion

We have performed the comparison of the latest version of IRI-2012 with global TEC data from JASON-1 satellite and with electron density profiles measured from ISRs at mid and high latitudes during the 2008–2009 solar minimum period. The comparison with global daily mean TEC shows that IRI underestimates the mean TEC by about 20–50% during the minimum period. The global TEC maps revealed specific details of the differences. The underestimation mostly occurs over the whole globe except for the daytime low-latitude region around the equatorial anomaly. The IRI prediction for the equatorial anomaly in the TEC maps significantly deviated from the JASON-1 TEC maps in terms of not only the magnitude of the anomaly crests but also their latitudinal locations in each hemisphere. Furthermore, the equatorial anomaly completely disappears in the evening in the IRI prediction. We

also found that the nighttime underestimation of IRI TEC is much stronger in the winter hemisphere than in the summer hemisphere. Considering the cooler and thinner thermosphere during the last solar minimum period, the resulting reduced recombination rate may be responsible for the larger electron densities of the measurement at night and in winter hemisphere than the IRI predictions. In other words, the nighttime ionosphere in IRI almost disappears in winter during the extremely low solar activity condition at all latitude regions.

The comparison of electron density profiles at mid and high latitudes reveals more specific differences between IRI and observations during the last solar minimum period. While the daytime IRI density profiles are relatively in good agreement with the ISR density profiles, the IRI model seems to significantly underestimate the high-latitude electron density at night, especially in winter, except around the F-region peak, which is consistent with the results of the TEC comparison.

The results of this study indicate that the most serious shortcomings in IRI-2012 appear to be the representations of the morphology of the equatorial anomaly and the nighttime ionosphere in winter, which are responsible for the overestimations and underestimations of the model, respectively.

Acknowledgments

This work was supported by the project PE16090 of Korea Polar Research Institute. The JASON-1 TEC data are obtained from the physical Oceanography Distributed Active Archive Center at the

NASA Jet propulsion Laboratory. The Millstone Hill radar data are obtained from the Madrigal Database at Haystack Observatory (<http://madrigal.haystack.mit.edu/madrigal/>). The EISCAT data are obtained from the EISCAT database in NIPR (<http://polaris.nipr.ac.jp/eiscat/eiscat-data/>). The IRI-2012 is available at GSFC NASA (<http://spdf.gsfc.nasa.gov/pub/models/iri/iri2012/>). We would like to thank Mr. Young-Bae Ham for his assistance in the data analysis for this work.

References

- Araujo-Pradere, E.A., Buresova, D., Fuller-Rowell, D.J., Fuller-Rowell, T.J., 2013. Initial results of the evaluation of IRI hmF2 performance for minima 22–23 and 23–24. *Adv. Space Res.* 51, 630–638.
- Azpilicueta, F., Brunini, C., 2009. Analysis of the bias between TOPEX and GPS vTEC determinations. *J. Geod.* 83, 121–127. <http://dx.doi.org/10.1007/s00190-008-0244-7>.
- Bilitza, D., 2000. The importance of EUV indices for the international reference ionosphere. *Phys. Chem. Earth* 25 (5), 515–521.
- Bilitza, D., 2009. Evaluation of the IRI-2007 model options for the topside electron density. *Adv. Space Res.* 44, 701–706.
- Bilitza, D., Reinisch, B.W., 2008. International reference ionosphere 2007: Improvements and new parameters. *Adv. Space Res.* 42, 599–609.
- Bilitza, D., Brown, S.A., Wang, M.Y., Souza, J.R., Roddy, P.A., 2012. Measurements and IRI model predictions during the recent solar minimum. *J. Atmos. Sol. Terr. Phys.* 86, 99–106.
- Bilitza, D., Altadill, D., Zhang, Y., Mertens, C., Truhlik, V., Richards, P., McKinnell, L.-A., Reinisch, B., 2014. The international reference ionosphere 2012 a model of international collaboration. *J. Space Weather Space Clim.* 4. <http://dx.doi.org/10.1051/swsc/2014004>.
- Brunini, C., Meza, A., Bosch, W., 2005. Temporal and spatial variability of the bias between TOPEX- and GPS-derived total electron content. *J. Geod.* 79, 175–188.
- Chen, Y., Liu, L., Wan, W., 2011. Does the F10.7 index correctly describe solar EUV flux during the deep solar minimum of 2007–2009? *J. Geophys. Res.* 116, A04304. <http://dx.doi.org/10.1029/2010JA016301>.
- Cherniakh, I.V., Zakharenkova, I.E., Dzyubanov, D.A., 2013. Accuracy of IRI profiles of ionospheric density and temperatures derived from comparisons to Kharkov incoherent scatter radar measurements. *Adv. Space Res.* 51, 639–646. <http://dx.doi.org/10.1016/j.asr.2011.12.022>.
- Codrescu, M.V., Beierle, K.L., Fuller-Rowell, T.J., Palo, S.E., Zhang, X., 2001. More total electron content climatology from TOPEX/Poseidon measurements. *Radio Sci.* 36, 325–333.
- Dettmering, D., Limberger, M., Schmidt, M., 2014. Using DORIS measurements for modeling the vertical total electron content of the Earth's ionosphere. *J. Geod.* 88, 1131–1143.
- Emmert, J.T., Lean, J.L., Picone, J.M., 2010. Record-low thermospheric density during the 2008 solar minimum. *Geophys. Res. Lett.* 37, L12102. <http://dx.doi.org/10.1029/2010GL043671>.
- Fu, L.L., Christensen, E.J., Yamarone, C.A., Lefevre, M., Menard, Y., Dorrer, M., Escudier, P., 1994. TOPEX/Poseidon mission overview. *J. Geophys. Res.* 99, 24369–24381.
- Ho, C.M., Wilson, B.D., Mannucci, A.J., Lindqwister, U.J., Yuan, D.N., 1997. A comparative study of ionospheric total electron content measurements using global ionospheric maps of GPS, TOPEX radar, and the Bent model. *Radio Sci.* 32, 1499–1512.
- Imel, D.A., 1994. Evaluation of the TOPEX/POSEIDON dual-frequency ionosphere correction. *J. Geophys. Res.* 99, 24895–24906.
- Jee, G., Schunk, R.W., Scherliess, L., 2005. Comparison of IRI-2001 with TOPEX TEC measurements. *J. Atmos. Sol. Terr. Phys.* 67, 365–380.
- Jee, G., Lee, H.-B., Solomon, S.C., 2014. Global ionospheric total electron contents (TECs) during the last two solar minimum periods. *J. Geophys. Res. Space Phys.* 119, 2090–2100. <http://dx.doi.org/10.1002/2013JA019407>.
- Jee, G., Lee, H.-B., Kim, Y.H., Chung, J.-K., Cho, J., 2010. Assessment of GPS global ionosphere maps (GIM) by comparison between CODE GIM and TOPEX/Jason TEC data: Ionospheric perspective. *J. Geophys. Res.* 115, A10319. <http://dx.doi.org/10.1029/2010JA015432>.
- Klenzing, J., Simões, F., Ivanov, S., Heelis, R.A., Bilitza, D., Pfaff, R., Rowland, D., 2011. Topside equatorial ionospheric density and composition during and after extreme solar minimum. *J. Geophys. Res.* 116, A12330. <http://dx.doi.org/10.1029/2011JA017213>.
- Lühr, H., Xiong, C., 2010. IRI-2007 model overestimates electron density during the 23/24 solar minimum. *Geophys. Res. Lett.* 37, L23101. <http://dx.doi.org/10.1029/2010GRL045430>.
- Lee, C.C., Reinisch, B.W., 2012. Variations in equatorial F2-layer parameters and comparison with IRI-2007 during a deep solar minimum. *J. Atmos. Sol. Terr. Phys.* 74, 217–223.
- Lee, H.-B., Jee, G., Kim, Y.H., Shim, J.S., 2013. Characteristics of global plasmaspheric TEC in comparison with the ionosphere simultaneously observed by Jason-1 satellite. *J. Geophys. Res. Space Phys.* 118, 935–946. <http://dx.doi.org/10.1002/jgra.50130>.
- Liu, L., Y. Chen, H. Le, Kurkin, V.I., Polekh, N.M., Lee, C.-C., 2011. The ionosphere under extremely prolonged low solar activity. *J. Geophys. Res.* 116, A04320. <http://dx.doi.org/10.1029/2010JA016296>.
- Liu, R.Y., Smith, P.A., King, J.W., 1983. A new solar index which leads to improved foF2 predictions using the CCIR Atlas. *Telecommun. J.* 50 (8), 408–414.
- Mannucci, A.J., Wilson, B.D., Yuan, D.N., Ho, C.H., Lindqwister, U.J., Runge, T.F., 1998. A global mapping technique for GPS-derived ionospheric total electron content measurements. *Radio Sci.* 33, 565–582.
- Ping, J., Matsumoto, K., Heki, K., Saito, A., Callahan, P., Potts, L., Shum, C.H., 2004. Validation of Jason-1 nadir ionosphere TEC using GEONET. *Mar. Geod.* 27, 741–752.
- Richmond, A.D., 1995. Ionospheric electrodynamic using magnetic apex coordinates. *J. Geomagn. Geoelectr.* 47, 191–212.
- Russell, C.T., Luhmann, J.G., Jian, L.K., 2010. How unprecedented a solar minimum? *Rev. Geophys.* 48, RG2004. <http://dx.doi.org/10.1029/2009RG000316>.
- Solomon, S.C., Qian, L., Burns, A.G., 2013. The anomalous ionosphere between solar cycles 23 and 24. *J. Geophys. Res. Space Phys.* 118, 6524–6535. <http://dx.doi.org/10.1002/jgra.50561>.
- Solomon, S.C., Woods, T.N., Didkovsky, L.V., Emmert, J.T., Qian, L., 2010. Anomalous low solar extreme-ultraviolet irradiance and thermospheric density during solar minimum. *Geophys. Res. Lett.* 37, L16103. <http://dx.doi.org/10.1029/2010GL044468>.
- Solomon, S.C., Qian, L., Didkovsky, L.V., Viereck, R.A., Woods, T.N., 2011. Causes of low thermospheric density during the 2007–2009 solar minimum. *J. Geophys. Res.* 116. <http://dx.doi.org/10.1029/2011JA016508>.
- Themens, D.R., Jayachandran, P.T., Nicolls, M.J., MacDougall, J.W., 2014. A top to bottom evaluation of IRI 2007 within the polar cap. *J. Geophys. Res. Space Phys.* 119, 6689–6703. <http://dx.doi.org/10.1002/2014JA020052>.
- Yasyukevich, Y.V., Afraimovich, E.L., Palamartchouk, K.S., Tatarinov, P.V., 2010. Cross testing of ionosphere models IRI-2001 and IRI-2007, data from satellite altimeters (Topex/Poseidon and Jason-1) and global ionosphere maps. *Adv. Space Res.* 46, 990–1007.
- Yizengaw, E., Moldwin, M.B., Galvan, D., Lijima, B.A., Komjathy, A., Mannucci, A.J., 2008. Global plasmaspheric TEC and its relative contribution to GPS TEC. *J. Atmos. Sol. Terr. Phys.* 70, 1541–1548.
- Yue, X., Schreiner, W.S., Rocken, C., Kuo, Y.-H., 2013. Validate the IRI2007 model by the COSMIC slant TEC data during the extremely solar minimum of 2008. *Adv. Space Res.* 51, 647–653.
- Zakharenkova, I.E., Cherniakh, I.V., Krankowski, A., Shagimuratov, I.I., 2015. Vertical TEC representation by IRI 2012 and IRI Plas models for European midlatitudes. *Adv. Space Res.* 55, 2070–2076.
- Zakharenkova, I.E., Krankowski, A., Bilitza, D., Cherniakh, I.V., Shagimuratov, I.I., Sieradzki, R., 2013. Comparative study of foF2 measurements with IRI-2007 model predictions during extended solar minimum. *Adv. Space Res.* 51, 620–629.
- Zhao, C., Shum, C.K., Yi, Y., Ge, S., Bilitza, D., Callahan, P., 2004. Accuracy assessment of the TOPEX/Poseidon ionosphere measurements. *Mar. Geod.* 27, 729–739.
- Zlotnicki, V., 1994. Correlated environmental correlations in TOPEX/Poseidon, with a note on ionospheric accuracy. *J. Geophys. Res.* 99, 24,907–24,914.